

Article

Removal of Arsenic from Water with Non-Thermal Plasma (NTP), Coagulation and Membrane Filtration

Jan O. Back ¹, Werner Stadlmayr ¹, Simon Jabornig ², Florian Winkler ², Karl Winkler ² and Marco Rupprich ^{1,*}

¹ Department of Environmental, Process & Energy Engineering, MCI-The Entrepreneurial School, Maximilianstrasse 2, 6020 Innsbruck, Austria; jan.back@mci.edu (J.O.B.); werner.stadlmayr@mci.edu (W.S.)

² SFC Umwelttechnik GmbH, Julius-Welser-Straße 15, 5020 Salzburg, Austria; jabornig@sfcu.at (S.J.); f.winkler@sfcu.at (F.W.); k.winkler@sfcu.at (K.W.)

* Correspondence: marco.rupprich@mci.edu; Tel.: +43-(0)512-2070-3210

Received: 11 September 2018; Accepted: 28 September 2018; Published: 3 October 2018



Abstract: Arsenic in drinking water resources and, especially, in groundwater, represents a severe health problem for millions of people in affected regions. This paper investigates a removal technology combining non-thermal plasma at a reaction time of 30 min, which has improved the downstream coagulation and the filtration efficiency. The results show removal rates of total arsenic over 98%. In addition, WHO limits of less than $10 \mu\text{g L}^{-1}$ could be achieved in both batch and continuous set-ups. A difference in effective over potential of the NTP reaction of 32 mV over a reaction using air as oxidant was calculated. Kinetic data of arsenic concentrations over time fitted a pseudo first-order reaction. The proposed process combination has shown to be a simple and energy-saving alternative compared to conventional oxidation and adsorption technologies by exploiting the ‘enhancer’ effect of ozone and other reactive oxygen species within the NTP.

Keywords: arsenic removal; non-thermal plasma; coagulation; membrane filtration; groundwater; ultrafiltration

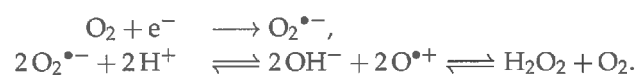
1. Introduction

Arsenic in groundwater resources represents a severe health issue for millions of people around the world. In Argentina, Bangladesh, Chile, China, India, Mexico, Serbia and the USA, wide areas are affected. The origin of arsenic can be either geogenic, i.e., volcanic activity and dissolution of minerals, or anthropogenic, i.e., mining and agriculture. Usually, in groundwater, the reduced form As(III) appears while, on the surface, water As(V) is present. As(V) can be classified as less mobile and, therefore, less toxic, because it is more likely to be adsorbed to metal hydroxides, i.e., iron or aluminium. The main pathway of intake by the human body is oral by drinking contaminated water. Health issues can be divided in acute and long term effects. Short-term symptoms are acute arsenic poisoning including vomiting, abdominal pain and diarrhoea. Long-term effects (arsenicosis) range from skin pigmentation, peripheral neuropathy, gastrointestinal symptoms, conjunctivitis, diabetes, renal system effects, enlarged liver, bone marrow depression, destruction of erythrocytes, high blood pressure, and cardiovascular diseases up to cancer. Even passing of arsenic through the placenta is reported and may lead to an increased risk for spontaneous abortion, stillbirth and preterm birth. As a consequence, the WHO lowered the limit for drinking water to $10 \mu\text{g L}^{-1}$ in order to decrease the daily dosage in affected areas to less than $3.0 \mu\text{g kg}^{-1}$ body weight per day [1].

Arsenic in its reduced form As(III) is far more poisonous than As(V) because of its high affinity to thiol-groups of proteins. As a result, many enzymatic pathways are affected or even blocked. Oral uptake of reduced or oxidized arsenic causes the same negative health effects because As(V) will be

quickly reduced to toxic As(III) in the body [2]. Literature on treatment and removal of arsenic from groundwater reports a wide range of technological approaches. Some of the technologies comprise oxidation steps to convert organic and trivalent arsenic As(III) to As(V) in a first step, e.g., dosage of KMnO_4 [3], photo catalytic oxidation on TiO_2 with UV light [4] or combination of ultrasonic and ultraviolet light [5]. Pentavalent arsenic generally shows higher affinity to surfaces, especially to iron hydroxide which is a result of a higher anionic charge. In this regard, it is comparable to the phosphoric acid/ortho-phosphate system [6]. Most of the investigated technologies so far use either adsorption or filtration for the final removal of arsenic. Adsorption materials reported in previous works are iron filings [7,8], granular ferric hydroxide [9], cupric oxide nanoparticles [10], manganese ore [11], iron cross-linked alginate [12], lignite, bentonite, shale and iron sand [13]. Microfiltration is only capable of separating precipitation products from iron or aluminium coagulation [14]. For direct removal of As(V), modified ultrafiltration (UF) [15] or nanofiltration membranes [3] have successfully been tested.

This study describes an innovative approach for arsenic removal from (ground)water through a combination of non-thermal plasma (NTP) treatment, coagulation, and UF, which will be compared to previously reported technologies. The aim of this work is to omit the dependency on oxidative chemicals which may cause additional harm to the environmental or high operating costs. Hence, the NTP technology, which is based on barrier discharge to form mainly negatively charged oxygen radicals, is used for oxidation purposes. Different oxygen ions (like $\text{O}_2^{\bullet-}$, O^\bullet , $\text{O}_2^{\bullet-}$ etc.) and ozone have been defined as reactive oxygen species (ROS) [16]. In the process, highly reactive ions are formed in ambient air, which are stabilized via cluster formation. Thus, their life span is long enough for them to be brought into the water treatment unit for further reaction. The formed compounds in water are mostly super oxide radical anions (in an excited state) which dissociate to oxygen radical ions [17] and subsequently to hydrogen peroxide via redox disproportionation [18]:



A pilot test series with different set-ups was carried out in order to test the following three hypotheses: (i) the oxidation potential of produced oxidants out of NTP is sufficient to convert As(III) to As(V), (ii) hollow fibre UF is suitable to remove the formed iron arsenate precipitations and (iii) the proposed process combination achieves WHO limits of less than $10 \mu\text{g L}^{-1}$ for arsenic in drinking water. This work will provide data for detailed process engineering and further research on this technology. Due to the positive results of this study, the authors conclude that this new treatment method could be a feasible and robust technology for arsenic removal from groundwater and other resources with low operating and maintenance costs.

2. Materials and Methods

2.1. Pilot Plant Set-Up

The individual tests were carried out in batches with a total volume of 60 L. Raw water was prepared with local tap water by adding different amounts of NaAsO_2 (0.05 mol L^{-1}) in order to adjust arsenic concentrations of $100\text{--}500 \mu\text{g L}^{-1}$. The general treatment process consisted of four main steps (Figure 1): (1) Filling of raw water into the reactor vessel; (2) Dosing of coagulant solution (FeCl_3 , $\text{Al}_2(\text{SO}_4)_3$) and co-current aeration, mixing and oxidation with non-thermal plasma (ionOXess, ionOXess GmbH, Innsbruck, Austria) or, in a blind test, just with ambient air, respectively. Subsequently, sedimentation was carried out (30 min for experiments A1–A5, 10 min for experiments A6–A12) (3) followed by the filtration of supernatant (4) with submerged UF hollow fiber membranes (C-MEMTM, SFC Umwelttechnik GmbH, Salzburg, Austria). Additionally, one series of tests was arranged as continuous system. In this set-up, steps 1 to 4 were performed co-currently in the same reactor tank with a retention time of 30 min (A13). Detailed process set-ups and dosing amounts are listed in Tables 1 and 2. Samples were taken from raw water and UF permeate for A6–A13

and, additionally, from the supernatant after sedimentation for A1–A5. Arsenic (as As_{total}) was measured on-site with test strips (Test Kit 2822800—EZ Arsenic; 0–500; 0–4000, Hach Lange GmbH, Vienna, Austria) and from retained samples according to ÖNORM EN ISO 17294-2 using inductively coupled plasma mass spectrometry (ICP-MS, Type 7500ce, Agilent Technologies, Vienna, Austria). Set-ups A1–A6 were carried out once, A7 and A8 twice and A9–A13 thrice. Turbidity and color were measured with a Hach DR/890 Colorimeter (Hach Lange GmbH, Vienna, Austria) and Hach 2100P ISO Turbidimeter (Hach Lange GmbH, Vienna, Austria).

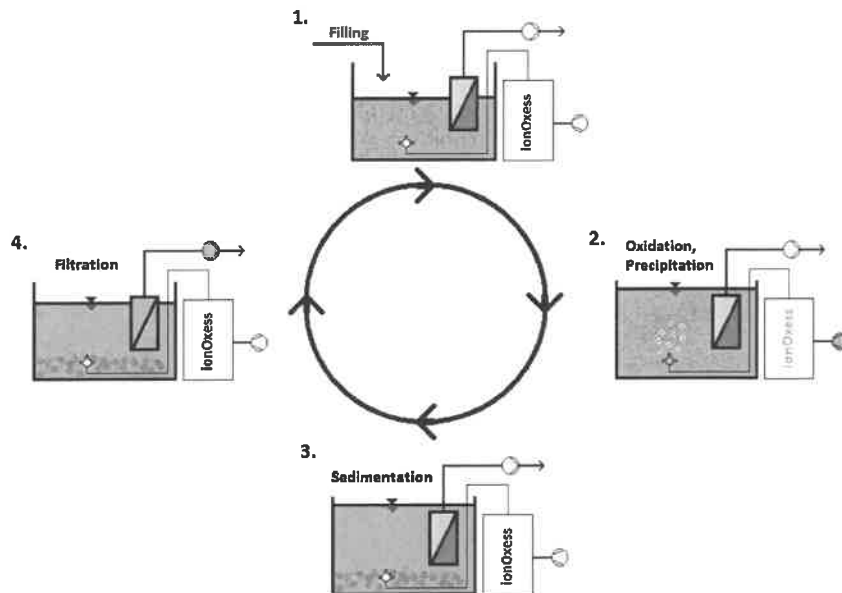


Figure 1. Process flow scheme of pilot tests: (1) Filling of raw water; (2) Dosing of coagulant and aeration (with or without NTP); (3) Sedimentation and (4) Filtration.

Table 1. Overview of process set-ups with coagulation and filtration only and a coagulation time of 30 min (no aeration).

Set-Up	As(III) / $\mu\text{g L}^{-1}$	Coagulation
A1	100	10 ppm Fe^{3+} as FeCl_3
A2	500	10 ppm Fe^{3+} as FeCl_3
A3	100	10 ppm Al^{3+} as $\text{Al}_2(\text{SO}_4)_3$
A4	100	50 ppm Fe^{3+} as FeCl_3
A5	100	25 ppm Fe^{3+} as FeCl_3 and 25 ppm Al^{3+} as $\text{Al}_2(\text{SO}_4)_3$

Table 2. Experimental results obtained in Experiments A6–A13. B and A stand for the conditions before and after the reaction, respectively. The values in the ‘As’-column are measured with the test strips and the values in the brackets with ICP-MS. The reduction was always calculated conservatively, i.e., using the highest value.

Set-Up (Oxidant)	Temp. / $^{\circ}\text{C}$	κ / $\mu\text{S cm}^{-1}$	pH	As / $\mu\text{g L}^{-1}$	Turbidity /NTU	Color /Pt-Co	Step (2) /min	As Reduction /%
A6 (air)	B	19.6	330	7.8	500	0.33	10	80
	A	20.6	371	7.1	100	0.45		
A7 (air)	B	17.9	333	7.8	500	0.32	30	80
	A	16.8	375	7.1	100	0.38		
A8 (air)	B	15.9	329	8	500	0.26	30	80
	A	16.1	375	6.9	100	0.26		

Table 2. Cont.

Set-Up (Oxidant)		Temp. /°C	κ / $\mu\text{S cm}^{-1}$	pH	As / $\mu\text{g L}^{-1}$	Turbidity /NTU	Color /Pt-Co	Step (2) /min	As Reduction /%
A8	B	16.8	334	7.9	500	0.26	24	60	80
	A	18.8	375	7.1	100	0.24	31		
(air)	B	18.0	328	7.8	500	0.29	35	60	80
	A	20.0	373	7.0	100	0.33	19		
A9 (NTP)	B	18.5	340	7.9	100	0.2	31	30	89
	A	18.2	367	7.0	10 (11)	0.38	28		
	B	19.2	339	7.9	100	0.26	28	30	88
	A	17.7	380	7.1	<10 (12)	0.26	28		
	B	16.5	338	7.9	100	0.21	34	30	90
	A	16.6	374	6.8	<10 (10)	0.2	41		
A10 (NTP)	B	16.4	324	7.7	500	0.51	31	10	>80
	A	17.5	367	7.0	50–100	0.18	34		
	B	16.8	324	7.9	500	0.4	20	10	>80
	A	18.0	364	7.1	50–100	0.34	29		
	B	17.2	322	7.9	500	0.24	35	10	>80
	A	17.3	363	7.0	50–100	0.28	22		
A11 (NTP)	B	18.8	331	7.9	500	0.65	22	20	>95
	A	17.9	370	7.0	10–25	0.48	30		
	B	17.4	374	7.8	500	0.77	39	20	>95
	A	17.5	372	7.0	10–25	0.25	31		
	B	17.5	339	7.9	500	0.45	30	20	95
	A	17.5	365	6.8	25	0.74	43		
A12 (NTP)	B	18.9	335	7.9	500	0.51	26	30	>98
	A	15.7	413	7.1	<10 (<5)	0.31	36		
	B	17.0	329	7.9	500	0.69	36	30	>98
	A	18.2	366	7.1	<10 (6.8)	0.56	50		
	B	16.3	332	8.0	500	0.23	34	30	>98
	A	16.7	365	7.0	<10 (<5)	0.5	35		
A13 (NTP)	B	15.6	350	7.9	500	0.29	35	30	97.5
	A	15.9	367	7.8	<10 (11)	0.39	38		
	B	19.2	338	7.7	500	0.23	36	30	97.5
	A	19.7	364	7.6	10 (11)	0.25	40		
	B	19.3	350	7.8	500	0.38	44	30	97.5
	A	19.8	372	7.9	<10 (11)	0.22	41		

2.2. Non-Thermal Plasma

Non-thermal plasma was generated via a barrier discharge at 3.2 kV and a frequency of 400 Hz with a plasma power of 6.4 W and a total plasma skid power of 50 W. The concentration of ions in the plasma air was determined with an ion-counter (Ionometer IM806, Umweltanalytik Holbach GmbH, Wadern, Germany). The concentration of negatively charged small ion clusters was around 52,000 ions per cm^3 and 76,000 ions per cm^3 for positively charged ions. Moreover, the concentration of ozone was around 90 ppm, which was measured with an ozone monitor (Model 106-M, ENVILYSE GmbH, Essen, Germany). Air was supplied with a membrane air pump (LA-28B, Nitto Kohki Europe, Steinenbronn, Germany) at 30 L min^{-1} . This yields an O_3 -flow of $0.19 \text{ mg O}_3 \text{ L}^{-1}$ (of air).

2.3. Coagulation and Precipitation

Coagulation with FeCl_3 and/or $\text{Al}_2(\text{SO}_4)_3$ after or co-currently to the NTP treatment was used to ensure precipitation and adsorption of oxidized arsenic inside or on iron or aluminium hydroxide flocs.

Adsorbed and precipitated arsenic was assumed to be accessible for removal through subsequent sedimentation and UF. FeCl_3 and/or $\text{Al}_2(\text{SO}_4)_3$ -solutions with a concentration of 41% and 17%, respectively, were added to the raw water to prepare concentration comparable with literature values between 10 to 50 ppm [14].

2.4. Ultrafiltration

As final polishing step after sedimentation, UF membranes were used to separate suspended slow-settling coagulation products and turbidity from water. The membrane module was submerged in the treatment tank. The active filtration area of one membrane module was around 6 m^2 . The applied filtration mode was dead-end (up to 10 min) with intermediate water back-flushing and air scouring (up to 30 s). The hollow fibre membrane inside the module was made of HDPE with a nominal pore size of $0.021 \mu\text{m}$. The trans-membrane suction pressure was between 0.2 to 0.3 bar. Clear water flux was in the range of 150 to $200 \text{ L m}^{-2} \text{ h}^{-1} \text{ bar}^{-1}$. After one batch, the membranes were manually cleaned with tap water and stored in clean water. Chemical cleaning was not applied during the testing period.

3. Results and Discussion

3.1. Influence of Different Coagulants (A1–A5)

In the first series of batch tests (A1–A5), the performance of different coagulants on arsenic adsorption/precipitation and its influence on the final result after sedimentation and UF without any aeration was investigated. The following three main results could be observed (Figure 2): (i) Generally, aluminium sulfate as coagulant showed lower adsorption rates in comparison to ferric chloride. (ii) The adsorption rate increases with increasing concentration of coagulant and (iii) WHO guidelines ($10 \mu\text{g L}^{-1}$) were exceeded by a factor of >2 even with best adsorption rates and following sedimentation and UF. The specific adsorption rate was highest at a As(III) concentration of $500 \mu\text{g L}^{-1}$ in the raw water. Removal of up to 80% of arsenic could be achieved.

The results agree with reported removal rates of arsenic using iron granulates [9]. In said study, the pseudo-first order reaction removes roughly 80% of the initial arsenic content within 30 min. Hence, in the present study, 30 min were used as typical reaction time. However, the lower excess of iron salts to arsenic in the present study does indicate a deviation from the pseudo-first order behaviour as can be seen in Figure 2. The removal rates depend on both arsenic and iron concentrations when comparing A1, A2, and A4, respectively. The increased adsorption rate of iron compared to aluminium could be explained by higher surface affinity to arsenic [2]. The contradictory result of higher arsenic concentration in the UF filtrate compared to raw water in A3 is not completely clear at the moment and might be due to experimental errors. Membrane filtration seems to be a key element not only for arsenic removal but also for aesthetic aspects of the treatment results, i.e., turbidity and color. The color in the supernatant was up to 122 Co/Pt units while it was only around 20 Co/Pt units in the UF permeate (A1–A2). Turbidity removal by UF was $>99\%$. The reddish color from non-settling iron coagulant which was still visible in the supernatant after 30 min of sedimentation could be removed by UF.

3.2. Influence of NTP on Arsenic Removal (A6–A13)

In a second series of batch tests (A6–A12) and in one continuous set-up (A13), the influence of oxidation, precipitation, and UF on arsenic removal was investigated. Oxidation of As(III) was conducted with both NTP (A9–A12, A13) and as a blind test with conventional aeration using ambient air (A6–A8). Figure 3a shows that the total arsenic concentration in the UF permeate drops rapidly through NTP treatment within reaction times of less than 20 min. The decline slows down and after 30 min arsenic concentration falls below the WHO limits. In addition, the quantification of As with test strips seems valid judging from a comparison to the ICP-MS method (see inset Figure 3b). For instance, for set-up, A12 measurements with test strips show concentrations smaller than $10 \mu\text{g L}^{-1}$, while the ICP-MS results were $5.6 \pm 1.0 \mu\text{g L}^{-1}$.

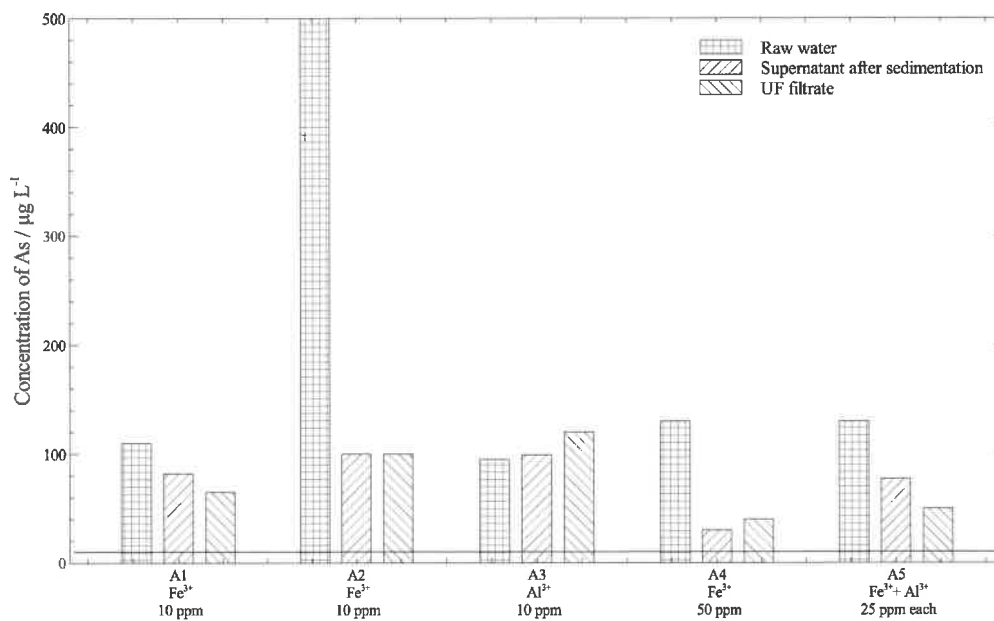


Figure 2. Arsenic removal efficiency after coagulation, sedimentation and UF filtration with different dosing rates of iron and aluminium coagulants for raw water spiked with 100 or 500 $\mu\text{g L}^{-1}$ of As(III). The green line shows the WHO limit of 10 $\mu\text{g L}^{-1}$.

Effluent concentration of aerated batches without NTP (A6 – A8) show that the removal remains at 80% over time, as previously confirmed in iron coagulation experiments (Figure 2). Compared to other studies about electro-chemical oxidation of arsenic, i.e., TiO_2 photo catalyst oxidation [4] or a combination of ultraviolet and ultrasound system [5] similar retention times of 10 to 30 min were required. Compared to electrocoagulation with 1 to 50 h significantly less treatment time was needed to achieve similar removal rates [14]. Literature data on high rate removal (>98%) of As(V) as AsO_4^- via iron coagulation was confirmed in NTP-oxidized batches [7,9]. These results suggest that no additional oxidizing chemicals are required for almost complete conversion of As(III) to As(V) when NTP is used. This could be an advantage compared to other hybrid membrane processes, in which a pre-oxidation step via potassium permanganate or sodium hypochlorite is necessary [3,19]. For future simplification of the process and reduced treatment time, arsenic removal with the same process principles—but as continuous system—was investigated in set-up A13. Similar to the batch set-up, total arsenic removal rates of 97.5% were measured. Simultaneous coagulant dosing and NTP treatment did not influence the final results. The apparent floc size was comparably smaller to the batch tests, which was probably the effect of intensive mixing without sedimentation. Nonetheless, arsenic seemed to be bound strongly on/inside the coagulant not only through adsorption but also as precipitated iron arsenate ($\text{FeAsO}_4 \cdot 2\text{H}_2\text{O}$).

A previous study by Yoon et al. [20] in which a combination of ozone with membrane filtration was used proved to be successful in As removal to comparable levels. However, the specific ozone concentrations as well as energy consumption (105 W for 4.0 L) were much higher than in the present study (50 W for 60 L). The ozone load in the carrier gas was 10 $\text{mg O}_3 \text{ L}^{-1}$ with pure O_2 as carrier gas, compared to 0.19 $\text{mg O}_3 \text{ L}^{-1}$ with ambient air as carrier gas in this study. Estimating the parameters under optimal conditions for the O_3 production with the ozone generator (LAB2B, Ozonia®, Duebendorf, Switzerland) used by Yoon et al., the total amount of O_3 introduced to the liquid phase after 20 min is 100 $\text{mg O}_3 \text{ L}^{-1}$. In the present study, the amount was only 3 $\text{mg O}_3 \text{ L}^{-1}$ after 30 min. The utilization of NTP equals a combination of ozone and other ROS, which seems to be overproportionally better than ozone alone. This ‘enhancer’ effect has already been reported in a previous study concerning the removal of organic micropollutants in wastewater via NTP [21].

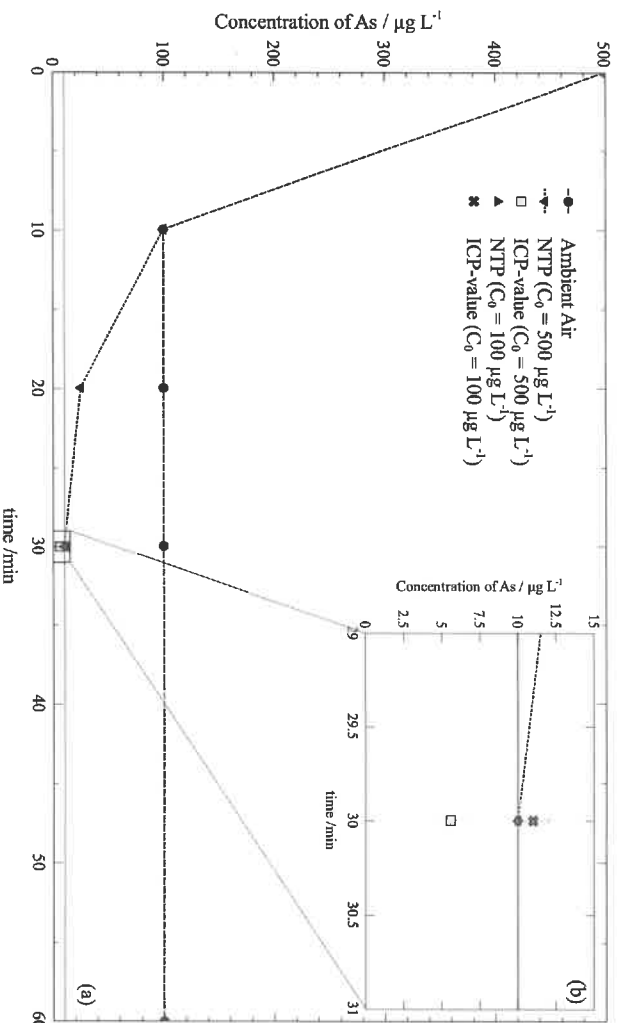


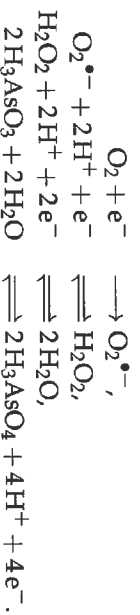
Figure 3. Concentration of remaining As(III) as a function of time and treatment method (a). The inset (b) is a magnification of the region of interest (i.e., As concentration around 10 µg L⁻¹). The values obtained with the test strips are in close proximity to the more accurate ICP-MS measurements. The green line shows the WHO limit of 10 µg L⁻¹.

3.3. Thermodynamic Considerations

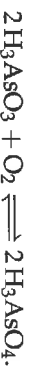
As observed in Table 2, the pH value drops from around 8 to around 7 pH units during As removal. This is partly due to the oxidation of the less acidic H₃AsO₃ (pK_{A,1} = 9.2; pK_{A,2} = 12.1; pK_{A,3} = 13.4) to the more acidic H₃AsO₄ (pK_{A,1} = 2.2; pK_{A,2} = 6.7; pK_{A,3} = 11.6) [20]. In addition, the addition of FeCl₃ might lower the pH. As the pH value approaches the pK_A value, the reaction stops, since *Eh* depends on the pH value. As can be seen in Figure 4, the reaction necessary for the removal of As (the oxidation from H₃AsO₃ to HAsO₄²⁻, while the latter corresponds to H₃AsO₄ below) becomes less likely with decreasing pH value, with a slope of -82 ± 17 mV/pH [22]. However, a reaction using NTP does still work better than one using only aeration (Figure 3). To get some insight into this, an effective over potential for both pathways was estimated using thermodynamic means. The following two reaction mechanisms are compared:



and



Since the first three reactions of the second mechanism can be summed up to yield the first reaction of the first mechanism, the overall reaction for both cases is:



Hence both reactions should share their thermodynamic properties, especially their value for the equilibrium constant *K*. However, experimental results show that, under both conditions, different resulting concentrations for H₃AsO₃ and H₃AsO₄ arise, even when starting from the same point.

Thus, one can try to determine an effective potential difference between both cases by applying thermodynamic formulae and working under the assumption that the difference can be summarized as an effective over potential. Superscript 1 stands for the first (with ambient air) and superscript 2 for the second mechanism (with NTP). The concentration or activity of H₂O and O₂ is assumed to be the same for both cases. It follows that

$$K_1 = \frac{[H_3AsO_4]_1^2}{[H_3AsO_3]_1^2 [O_2]}$$

and

$$K_2 = \frac{[H_3AsO_4]_2^2}{[H_3AsO_3]_2^2 [O_2]}$$

Using

$$\Delta G^\circ = -RT \ln K = -zF\Delta E^\circ, \tag{1}$$

one can calculate an effective ΔE° :

$$\Delta E_{i, \text{Eff.}}^\circ = \frac{RT}{zF} \ln K_i. \tag{2}$$

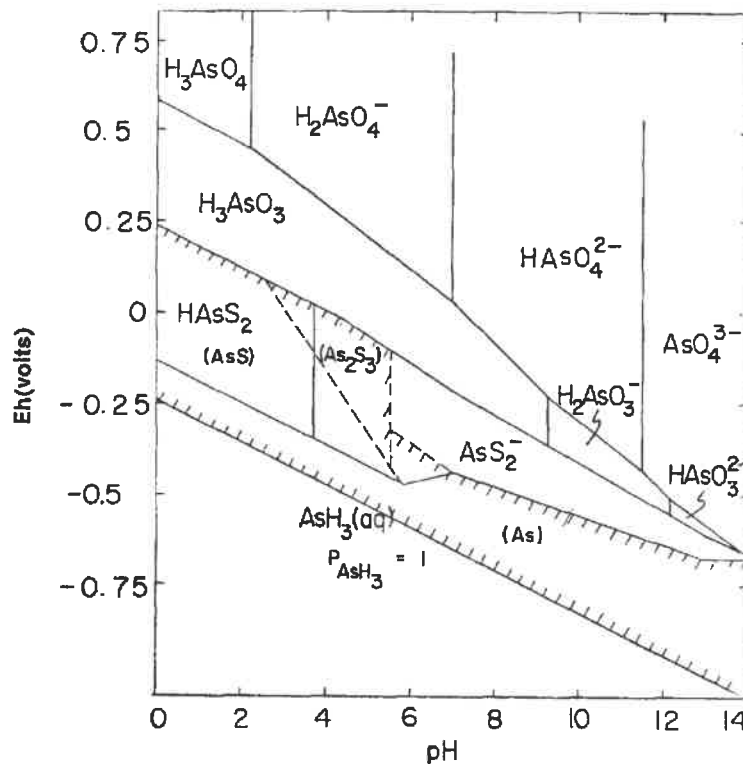


Figure 4. The Eh-pH diagram for As at 25°C and one atmosphere with total arsenic $1 \times 10^{-5} \text{ mol L}^{-1}$. Reprinted from [23], with permission from Elsevier.

The effective potential difference can thus be calculated as

$$\Delta \Delta E_{\text{Eff.}}^\circ = \Delta E_{2, \text{Eff.}}^\circ - \Delta E_{1, \text{Eff.}}^\circ. \tag{3}$$

Inserting the equations for both terms yields

$$\Delta \Delta E_{\text{Eff.}}^\circ = \frac{RT}{zF} \ln K_2 - \frac{RT}{zF} \ln K_1 = \frac{RT}{zF} \ln \left(\frac{K_2}{K_1} \right),$$

which, inserting the actual values ($z = 4$), in turn, can be rewritten to

$$\Delta\Delta E_{\text{Eff}}^{\circ} = 0.0128 \text{ J C}^{-1} \ln \left(\frac{[\text{H}_3\text{AsO}_4]_2 [\text{H}_3\text{AsO}_3]_1}{[\text{H}_3\text{AsO}_4]_1 [\text{H}_3\text{AsO}_3]_2} \right).$$

Experimental values were obtained by measuring the mass concentration of As in $\mu\text{g L}^{-1}$ which can be related to $[\text{H}_3\text{AsO}_3]$ before and after the treatment step. Assuming that the removed As(III) was oxidized to As(V), the calculated concentrations were $c_{\text{H}_3\text{AsO}_4,1} = 5.34 \mu\text{mol L}^{-1}$, $c_{\text{H}_3\text{AsO}_3,1} = 1.33 \mu\text{mol L}^{-1}$, $c_{\text{H}_3\text{AsO}_4,2} = 6.54 \mu\text{mol L}^{-1}$ and $c_{\text{H}_3\text{AsO}_3,2} = 0.133 \mu\text{mol L}^{-1}$. Inserting the values leads to

$$\Delta\Delta E_{\text{Eff}}^{\circ} = 0.0128 \text{ J C}^{-1} \ln \left(\frac{6.54 \mu\text{mol L}^{-1} \cdot 1.33 \mu\text{mol L}^{-1}}{5.34 \mu\text{mol L}^{-1} \cdot 0.133 \mu\text{mol L}^{-1}} \right) = 0.032 \text{ V}.$$

Consequently, the difference in the two reaction mechanisms can be compared to a difference in effective over potential of 32 mV. As shown in Figure 4, this means that one pathway is still working, even when shifted to lower pH values, yielding better As removal. Since the slope is rather steep, the expected change in pH is rather low (roughly 0.3 pH units) and cannot be resolved experimentally. Thus, while both oxidation mechanisms will work worse in a lower pH environment, the mechanism utilizing NTP will work better due to the 32 mV difference in effective over potential and, consequently, the shift upwards in direction of the As(V)-species in Figure 4. Further experiments could consider the possibility of keeping the pH value above 7.5 or more for enhanced oxidation.

3.4. Kinetic Considerations

The kinetics of the mechanism were compared to results obtained by Yoon et al. [20]. Since their study was concerned with a 'pure ozone mechanism', the results are not directly comparable. While Yoon et al. derived a second-order reaction kinetic with $k_2 = 5.5 \times 10^5 \text{ L mol}^{-1} \text{ s}^{-1}$, the results shown in this study are in favor of a pseudo-first order reaction kinetic with $k_1 = 2.7 \times 10^{-3} \text{ s}^{-1}$ (see Figure 5). A second-order regression using this data would yield a $k_2 = 1.3 \times 10^3 \text{ L mol}^{-1} \text{ s}^{-1}$. This can be explained by ozone and ROS being continuously replenished during the reaction.

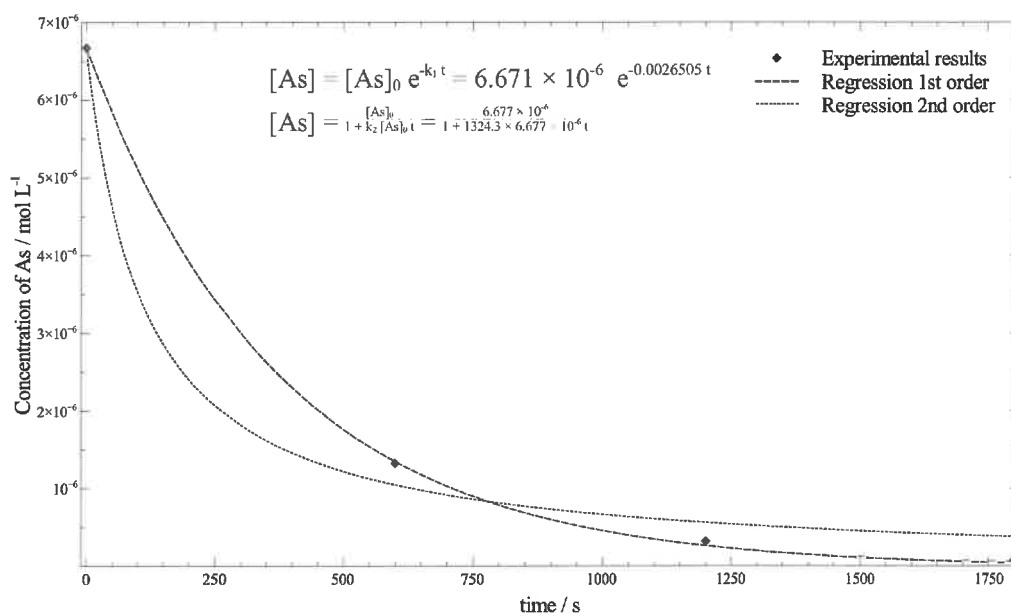


Figure 5. Kinetic data and first and second order regression.

4. Conclusions

Three different methods were compared concerning the ability to remove arsenic from water: Firstly, precipitation/coagulation and UF (A1–A5), secondly precipitation/coagulation, UF, and oxidation with ambient air (A6–A8), and finally precipitation/coagulation, UF, and oxidation with NTP (A9–A13). The latter has best succeeded in the removal of arsenic from drinking water and the WHO requirements of concentrations less than $10 \mu\text{g L}^{-1}$ have been achieved. NTP was more efficient in converting As(III) to As(V) than ambient air. The studied process is an energy-efficient system, which can easily be utilized for decentralised water purification in e.g., rural areas. Due to the ‘enhancer’ effect, low ozone concentrations suffice for arsenic removal and, consequently, no ozone filters would be required in a possible application. Future experiments should focus on control of pH value, energy consumption, scale-up, and understanding the mechanism behind the ‘enhancer’ effect.

Author Contributions: Conceptualization, S.J. and M.R.; Data curation, W.S. and M.R.; Formal analysis, W.S. and M.R.; Investigation, S.J. and M.R.; Methodology, J.O.B., F.W. and K.W.; Project Administration, S.J. and M.R.; Resources, S.J. and M.R.; Supervision, S.J. and M.R.; Validation, K.W.; Visualization, J.O.B., F.W. and M.R.; Writing—Original Draft, J.O.B., F.W. and K.W.; Writing—Review and Editing, W.S. and M.R. Funding Acquisition, no external funding received.

Funding: This research received no external funding.

Conflicts of Interest: The authors declare no conflict of interest. The founding sponsors had no role in the design of the study; in the collection, analyses, or interpretation of data; in the writing of the manuscript, and in the decision to publish the results.

Abbreviations

The following abbreviations are used in this manuscript:

ICP-MS	Inductively Coupled Plasma Mass Spectrometry
NTP	Non-Thermal Plasma
ROS	Reactive Oxygen Species
UF	Ultrafiltration
WHO	World Health Organisation

References

1. World Health Organization (WHO); Public Health and Environment (Eds.) *Exposure to Arsenic: A Major Public Health Concern*; WHO Document Production Services: Geneva, Switzerland, 2010.
2. Dekant, W.; Vamvakas, S. *Toxikologie für Chemiker und Biologen*, 1st ed.; Spektrum Lehrbuch, Spektrum Akad. Verl.: Heidelberg, Germany, 1995.
3. Sen, M.; Manna, A.; Pal, P. Removal of arsenic from contaminated groundwater by membrane-integrated hybrid treatment system. *J. Membr. Sci.* **2010**, *354*, 108–113. [CrossRef]
4. Guan, X.; Du, J.; Meng, X.; Sun, Y.; Sun, B.; Hu, Q. Application of titanium dioxide in arsenic removal from water: A review. *J. Hazard. Mater.* **2012**, *215–216*, 1–16. [CrossRef] [PubMed]
5. Cui, M.; Jang, M.; Ibrahim, S.; Park, B.; Cho, E.; Khim, J. Arsenite removal using a pilot system of ultrasound and ultraviolet followed by microfiltration. *Ultrason. Sonochem.* **2014**, *21*, 1527–1534. [CrossRef] [PubMed]
6. Jekel, M.; Amy, G.L. Arsenic removal during drinking water treatment. In *Interface Science in Drinking Water Treatment—Theory and Application*; Elsevier: London, UK; Amsterdam, The Netherlands, 2006; Volume 10, pp. 193–206. [CrossRef]
7. Cheng, Z.; van Geen, A.; Louis, R.; Nikolaidis, N.; Bailey, R. Removal of Methylated Arsenic in Groundwater with Iron Filings. *Environ. Sci. Technol.* **2005**, *39*, 7662–7666. [CrossRef] [PubMed]
8. Leupin, O.X.; Hug, S.J. Oxidation and removal of arsenic (III) from aerated groundwater by filtration through sand and zero-valent iron. *Water Res.* **2005**, *39*, 1729–1740. [CrossRef] [PubMed]
9. Banerjee, K.; Amy, G.L.; Prevost, M.; Nour, S.; Jekel, M.; Gallagher, P.M.; Blumenschein, C.D. Kinetic and thermodynamic aspects of adsorption of arsenic onto granular ferric hydroxide (GFH). *Water Res.* **2008**, *42*, 3371–3378. [CrossRef] [PubMed]

10. Reddy, K.J.; McDonald, K.J.; King, H. A novel arsenic removal process for water using cupric oxide nanoparticles. *J. Colloid Interface Sci.* **2013**, *397*, 96–102. [CrossRef] [PubMed]
11. Chakravarty, S.; Dureja, V.; Bhattacharyya, G.; Maity, S.; Bhattacharjee, S. Removal of arsenic from groundwater using low cost ferruginous manganese ore. *Water Res.* **2002**, *36*, 625–632. [CrossRef]
12. Singh, P.; Singh, S.K.; Bajpai, J.; Bajpai, A.K.; Shrivastava, R.B. Iron crosslinked alginate as novel nanosorbents for removal of arsenic ions and bacteriological contamination from water. *J. Mater. Res. Technol.* **2014**, *3*, 195–202. [CrossRef]
13. Mar, K.K.; Karnawati, D.; Sarto; Putra, D.; Igarashi, T.; Tabelin, C.B. Comparison of Arsenic Adsorption on Lignite, Bentonite, Shale, and Iron Sand from Indonesia. *Procedia Earth Planet. Sci.* **2013**, *6*, 242–250. [CrossRef]
14. Mólgora, C.C.; Domínguez, A.M.; Avila, E.M.; Drogui, P.; Buelna, G. Removal of arsenic from drinking water: A comparative study between electrocoagulation-microfiltration and chemical coagulation-microfiltration processes. *Sep. Purif. Technol.* **2013**, *118*, 645–651. [CrossRef]
15. Lohokare, H.R.; Muthu, M.R.; Agarwal, G.P.; Kharul, U.K. Effective arsenic removal using polyacrylonitrile-based ultrafiltration (UF) membrane. *J. Membr. Sci.* **2008**, *320*, 159–166. [CrossRef]
16. Knoll, M.; Eichmeier, J.; Schön, R.; Hoegl, A.; Hock, A.; Schmeer, H. Properties, measurement, and bioclimatic action of “small” multimolecular atmospheric ions. In *Advances in Electronics and Electron Physics*; Elsevier: New York, NY, USA, 1964; Volume 19, pp. 177–254.
17. Goldstein, N.I.; Goldstein, R.N.; Merzlyak, M.N. Negative air ions as a source of superoxide. *Int. J. Biometeorol.* **1992**, *36*, 118–122. [CrossRef]
18. Challenger, O.; Braven, J.; Harwood, D.; Rosén, K.; Richardson, G. Negative air ionisation and the generation of hydrogen peroxide. *Sci. Total Environ.* **1996**, *177*, 215–219. [CrossRef]
19. Guzmán, A.; Nava, J.L.; Coreño, O.; Rodríguez, I.; Gutiérrez, S. Arsenic and fluoride removal from groundwater by electrocoagulation using a continuous filter-press reactor. *Chemosphere* **2016**, *144*, 2113–2120. [CrossRef] [PubMed]
20. Yoon, Y.; Hwang, Y.; Ji, M.; Jeon, B.H.; Kang, J.W. Ozone/membrane hybrid process for arsenic removal in iron-containing water. *Desalin. Water Treat.* **2011**, *31*, 138–143. [CrossRef]
21. Back, J.O.; Obholzer, T.; Winkler, K.; Jabornig, S.; Rupprich, M. Combining ultrafiltration and non-thermal plasma for low energy degradation of pharmaceuticals from conventionally treated wastewater. *J. Environ. Chem. Eng.* **2018**. [CrossRef]
22. Yan, X.P.; Kerrich, R.; Hendry, M.J. Distribution of arsenic (III), arsenic (V) and total inorganic arsenic in porewaters from a thick till and clay-rich aquitard sequence, Saskatchewan, Canada. *Geochim. Cosmochim. Acta* **2000**, *64*, 2637–2648. [CrossRef]
23. Ferguson, J.F.; Gavis, J. A review of the arsenic cycle in natural waters. *Water Res.* **1972**, *6*, 1259–1274. [CrossRef]



